ELSEVIER

Chemical Geology 230 (2006) 105–123

CHEMICAL GEOLOGY
INCLUDING
ISOTOPE GEOSCIENCE

www.elsevier.com/locate/chemgeo

Rare earth and trace elements of microbialites in Upper Jurassic coral- and sponge-microbialite reefs

Nicolas Olivier [a,b,*], Maud Boyet [c,d]

[a] Université Claude Bernard Lyon1, UMR CNRS 5125 PEPS, 2 rue Raphaël Dubois, 69622 Villeurbanne cedex, France
[b] Université de Nantes, UMR CNRS 6112 LPGN, 2 rue de la Houssinière PB 92208, 44322 Nantes cedex 3, France
[c] Ecole normale supérieure de Lyon, UMR CNRS 5570, 46 allée d'Italie, 69364 Lyon cedex 07, France
[d] Carnegie Institution of Washington, Dept. of Terrestrial Magnetism, 5241 Broad Branch Rd., N.W., Washington, D.C. 20015, USA

Received 20 January 2005; received in revised form 30 September 2005; accepted 5 December 2005

Abstract

Major, trace (Y, Zr, Pb, Th and U), rare earth element (REE) and Sm–Nd isotope analyses were carried out on microbialites and detrital carbonate sediments collected in Upper Jurassic coral- and sponge-microbialite reef settings. Selected bioconstructions developed in various palaeogeographic settings and depositional environments on northwestern Tethys and eastern Atlantic margins: pure carbonate lagoon, carbonate-dominated deep shelf to epicontinental basin and mixed carbonate-siliciclastic shallow ramp and lagoon. The proximity to terrigenous sources directly controlled REE patterns of carbonate samples. Lateral and intra-reef sediments, and to a lesser degree stromatolitic microbial crusts, are more susceptible to contamination by terrigenous material than are microbialites of thrombolitic fabric. In mixed carbonate-siliciclastic settings, microbialites display a flat shale-normalized REE pattern. In pure carbonate lagoonal settings, microbialites have shale-normalized REE patterns similar to those of modern seawaters with a negative Ce anomaly [(Ce/Ce*) up to 0.14], positive La and Gd anomalies, and light REE depletion relative to heavy REE. These data imply that similar REE chemistry than modern seawater already occurred on the northwestern Tethys margin at the Upper Jurassic. Strong negative Ce anomalies (<0.4) imply microbialite formation in well-oxygenated seawaters both in coral reefs of pure carbonate lagoonal environments (Pagny-sur-Meuse) and sponge bioherms of deep-shelf settings (Plettenberg). Absence of positive Ce anomalies rules out an influence of alkaline and high-pH seawaters. Thus, REE patterns and Nd isotopic signatures, which are in perfect agreement with existing results for Tethysian seawater, confirm that microbialites can be used as proxies of palaeoenvironmental seawater chemical characteristics.

Keywords: Rare earth elements; Nd isotopes; Upper Jurassic seawater; Microbialites; Coral and sponge reefs; Palaeoenvironment

1. Introduction

Trace and rare earth element (REE) concentrations recorded in both carbonate and phosphate sediments have been used to obtain information on marine palaeoenvironments (e.g. Wright et al., 1987; Liu et al., 1988; Murray et al., 1991). However, many prospective proxies for ancient seawater REE reconstructions may

* Corresponding author. Université Claude Bernard Lyon1, UMR CNRS 5125 PEPS, 2 rue Raphaël Dubois, 69622 Villeurbanne cedex, France.
E-mail addresses: Nicolas.Olivier@univ-lyon1.fr (N. Olivier), boyet@dtm.ciw.edu (M. Boyet).

0009-2541/$ - see front matter © 2005 Elsevier B.V. All rights reserved.
doi:10.1016/j.chemgeo.2005.12.002

suffer from a large variety of problems (e.g. vital effects or diagenetic alteration) that obscure the original seawater signature (German and Elderfield, 1990; Holser, 1997). Recently, Webb and Kamber (2000) have demonstrated that modern carbonate-type sediments of microbial origin, the microbialites, incorporate REE from seawater with uniform and high partition coefficients, and thus was a reliable proxy for ancient seawater REE chemistry. Microbial carbonates were largely abundant throughout Precambrian times and periodically widespread during the Phanerozoic, before being marked by a net decline after 150 My (Wood, 1999; Webb, 2001; Arp et al., 2001; Riding, 2000, 2005). The abundance of microbial carbonates has been interpreted as reflecting changes in seawater chemistry (i.e. in the saturation state with respect to $CaCO_3$ minerals) that determines the extent of microbial calcification (Riding and Liang, 2005a). The decreased occurrence of microbial carbonates after 150 My could be linked to the Cretaceous radiation of coccolithophore algae and globigerine foraminifers, which changed the seawater chemistry by depressing the saturation state (Riding and Liang, 2005b; Riding, 2005). Different studies of ancient sedimentary phosphates also suggest that pre-Cenozoic seawater had a different REE pattern from today, marked by a depletion in the heavy REE (e.g. McArthur and Walsh, 1984; Grandjean et al., 1987, 1988; Grandjean-Lécuyer et al., 1993; Ilyin, 1998; Picard et al., 2002; Lécuyer et al., 2004). However, such a change in seawater REE chemistry during the Cretaceous period is still matter of debate (Shields and Webb, 2004).

The Upper Jurassic is marked by a peak in the abundance of microbialites that developed in a wide range of environments, from shallow proximal platforms to deep epicontinental basins (Leinfelder et al., 1993; Dromart et al., 1994; Leinfelder and Schmid, 2000). Upper Jurassic microbialites thus can constrain the seawater REE chemistry before the radiation of the Cretaceous plankton. On the other hand, the physico-chemical parameters controlling the formation of Upper Jurassic microbialites are still misunderstood. The amount of nutrients present in the water column is generally proposed to be the dominant controlling factor; however, oxygenation, pH level and alkalinity are also invoked to favour their development (Reitner and Neuweiler, 1995; Leinfelder et al., 1996; Schmid, 1996; Bertling and Insalaco, 1998; Dupraz and Strasser, 1999, 2002; Leinfelder and Schmid, 2000; Leinfelder, 2001; Webb, 2001).

Major, trace elements (Y, Zr, Pb, Th and U), REE and Nd isotopes were analysed on microbialites from various Upper Jurassic reef ecosystems located in different palaeoenvironments on northwestern Tethys and eastern Atlantic margins. Microbialites were sampled in coral reefs from a pure carbonate lagoon, sponge bioherms from a carbonate-dominated deep shelf to

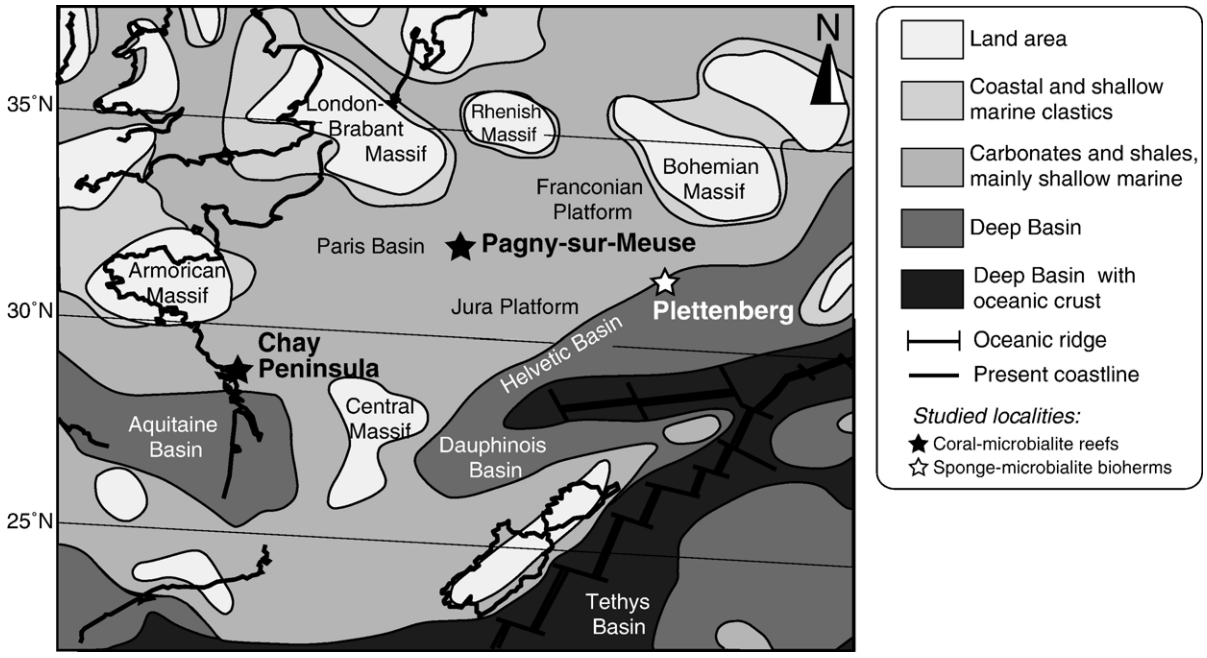

Fig. 1. Location of studied Oxfordian coral- and sponge-microbialite reefs (Pagny-sur-Meuse and Plettenberg, respectively) and Kimmeridgian coral-microbialite reefs (Chay Peninsula) on a palaeogeographic map during the Upper Jurassic (modified after Ziegler, 1990; Carpentier, 2004).

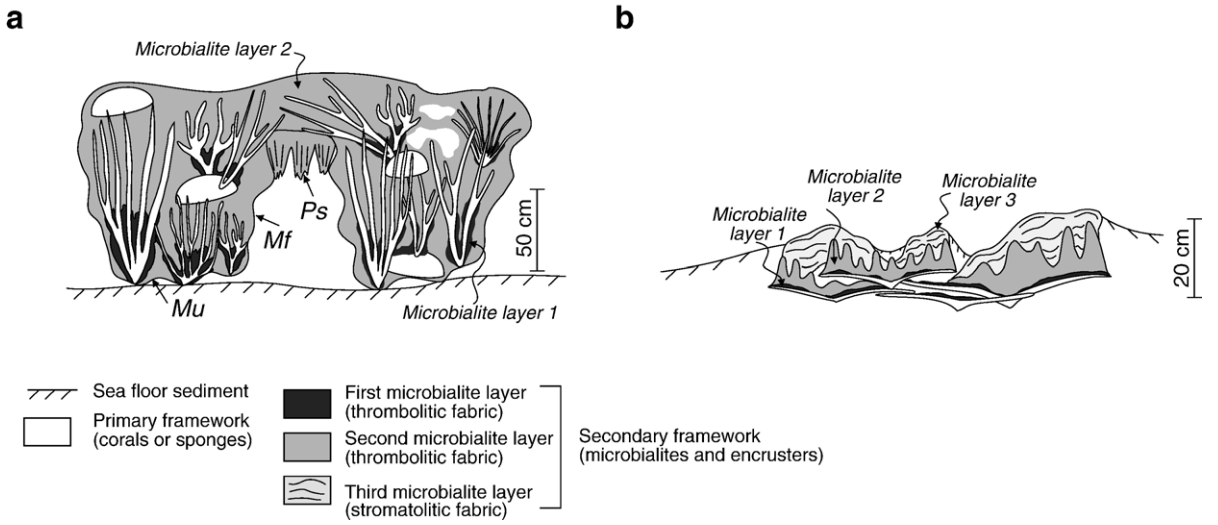

Fig. 2. Schematic sketches showing the architecture of (a) coral- and (b) sponge-microbialite bioconstructions in which analysed microbialites were collected. The microbialites formed on a previous skeletal framework mainly made of corals or sponges. The microbialite crust is composed of two and three layers in coral reefs and sponge bioherms, respectively. Abbreviations: Ps, pseudostalactite microbialites; Mu, mammilated microbialites of bioherm underside; Mf, mammilated microbialites of bioherm flanks. See text for more explanations.

epicontinental basin and coral reefs from mixed carbonate-siliciclastic lagoon and shallow ramp. Analyses were performed on different types of microbialites, as well as lateral and intra-reef sediments. This work focuses on the use of microbialite-type carbonate to reconstruct the REE seawater signature and the factors controlling microbialites formation.

2. Materials and methods

2.1. Samples and geological framework

Samples come from coral- and sponge-microbialite reef environments of the Upper Jurassic (Oxfordian and Kimmeridgian ages) located in different palaeoenvironments on northwestern Tethys and eastern Atlantic margins (Fig. 1). Among 17 analysed samples, 14 are microbialites, i.e. "organosedimentary deposits that have accreted as a result of a benthic microbial community trapping and binding detrital sediment and/or forming the locus of mineral precipitation" (Burne and Moore, 1987). In studied bioconstructions, microbialites form centimeter-scale crusts at the surface of a primary framework made up of sponges or corals (Fig. 2). Microbialite crusts are generally two-layered in coral reefs and three-layered in sponge bioherms (Olivier, 2004). In order to enlarge our data set and compare it to microbialites, three samples were collected from non-bioconstructed lateral or intra-reef carbonate sediments. Reef settings are described briefly below and their main characteristics (age, lithology and depositional environments) are summarized in Table 1. For more detailed information on sedimentological, palaeontological and palaeoenvironmental contexts, the reader can refer to previous literature on the Chay Peninsula (Hantzpergue, 1991; Olivier et al., 2003), Pagny-sur-Meuse (Geister

Table 1
Brief lithological descriptions of the lateral deposits of coral- and sponge-microbialite reefs and their depositional environments (after Olivier et al., 2003, 2004a,b)

Locality	Samples	Age	Lithology of reef lateral deposits	Depositional environment
Chay Peninsula	Cp1–4	Lower Kimmeridgian Cymodoce Zone	Wackestone→Packstone	Mixed carbonate-siliciclastic shallow ramp
Plettenberg	Pt1–7	Upper Oxfordian Bimammatum Zone	Wackestone	Carbonate-dominated deep shelf
Pagny-sur-Meuse	Pm6	Upper Oxfordian Bimammatum Zone	Packstone	Mixed carbonate-siliciclastic lagoon
	Pm1–5	Middle Oxfordian Transversarium Zone	Wackestone→Packstone	Pure carbonate lagoon

Table 2
Major and trace element contents of 17 Upper Jurassic carbonates, including microbialites, lateral and intra-reef sediments

Location	Chay Peninsula				Plettenberg							Pagny-sur-Meuse						Standard
Sample	Cp1	Cp2	Cp3	Cp4	Pt1	Pt2	Pt3	Pt4	Pt5	Pt6	Pt7	Pm1	Pm2	Pm3	Pm4	Pm5	Pm6	BHVO
Type	Microb.	Microb.	Microb.	Microb.	Microb.	Microb.	Microb.	Microb.	Microb.	Int. sed.	Lat. sed.	Microb.	Microb.	Microb.	Microb.	Int. sed.	Microb.	
	Layer 2	Layer 2	Layer 2	Layer 2	Layer 1	Layer 2	Layer 2	Layer 3	Layer 3			Layer 2	Layer 2	Layer 2	Layer 2		Layer 2	
Age	Kim.	Kim.	Kim.	Kim.	Oxf.	Oxf.	Oxf.	Oxf.	Oxf.	Oxf.	Oxf.	Oxf.	Oxf.	Oxf.	Oxf.	Oxf.	Oxf.	
Majors[a]*—whole rock*																		
SiO_2	3.78	4.87	3.98	3.91	3.53	5.50		3.32		8.68	3.16	0.20	0.09	0.16		0.13	7.10	
Al_2O_3	1.14	1.54	1.56	1.28	1.07	1.70		1.10		3.18	1.21	0.04	0.05	0.05		0.04	1.68	
Fe_2O_3	0.73	0.75	0.45	0.57	0.45	0.61		0.59		0.93	0.59	0.04	0.04	0.04		0.04	0.80	
MnO	0.03	0.03	0.03	0.03	0.03	0.03		0.04		0.05	0.02	–	–	–		0.00	0.05	
MgO	1.19	1.22	1.18	1.23	1.29	1.44		1.46		1.54	1.31	0.89	0.89	0.83		0.83	1.53	
CaO	92.84	91.23	92.48	92.72	93.40	90.27		93.21		85.11	93.42	98.75	98.84	98.83		98.89	88.28	
Na_2O	0.09	0.09	0.10	0.09	0.05	0.09		0.11		0.12	0.09	0.05	0.05	0.05		0.05	0.08	
K_2O	0.07	0.12	0.10	0.07	0.07	0.24		0.07		0.19	0.07	–	–	–		0.00	0.31	
TiO_2	0.07	0.09	0.07	0.07	0.05	0.07		0.05		0.12	0.05	0.02	0.02	0.02		0.02	0.12	
P_2O_5	0.05	0.05	0.03	0.03	0.05	0.05		0.05		0.08	0.09	0.02	0.02	0.02		0.02	0.05	
L.O.I	42.46	42.08	42.39	42.47	42.60	41.86		42.63		40.51	42.65	43.76	43.68	43.67		43.73	41.36	
Total	100.59	100.67	100.82	100.53	99.98	99.83		99.02		99.91	99.15	99.93	99.84	100.27		99.47	100.45	
Traces—whole rock																		
La		3.53		3.29		5.24			3.82		7.02	0.787		0.735		1.12	4.54	15.27
Ce		6.59		6.35		4.64			5.07		4.24	0.149		0.176		0.248	8.649	38.59
Pr		0.738		0.742		0.799			0.702		1.015	0.074		0.075		0.104	1.030	5.20
Nd		2.75		2.82		3.01			2.71		4.41	0.305		0.299		0.400	4.013	24.5
Sm		0.500		0.606		0.582			0.500		0.814	0.050		0.062		0.059	0.819	5.82
Eu		0.123		0.117		0.130			0.109		0.190	0.015		0.014		0.015	0.167	2.07
Gd		0.427		0.478		0.579			0.390		1.002	0.073		0.089		0.097	0.608	6.21
Tb		0.074		0.080		0.103			0.078		0.157	0.012		0.013		0.012	0.130	0.90
Dy		0.477		0.501		0.648			0.468		0.959	0.083		0.092		0.097	0.699	5.54
Y		1.68		1.83		3.06			1.99		5.16	1.29		1.01		1.19	1.56	0.97
Ho		0.096		0.087		0.148			0.098		0.234	0.027		0.021		0.026	0.150	2.40
Er		0.264		0.276		0.409			0.249		0.591	0.080		0.079		0.072	0.399	0.320
Tm		0.036		0.037		0.064			0.035		0.095	0.006		0.007		0.011	0.053	1.87
Yb		0.252		0.266		0.332			0.197		0.446	0.065		0.061		0.044	0.358	0.280
Lu		0.033		0.037		0.054			0.024		0.076	0.008		–		–	0.048	25.43

Zr		5.25		5.07		3.00			2.96		2.41	0.338		0.099		0.143	7.235	174.2
Hf		0.432		0.249		0.166			0.143		0.123	0.071		0.056		–	0.438	4.22
Nb		1.18		1.28		0.732			1.14		0.776	1.60		0.028		0.019	1.438	
Ta		0.383		0.237		–			0.493		0.118	1.909		0.073		–	0.081	1.19
Pb		3.29		0.934		1.17			0.677		1.84	0.106		0.137		0.108	1.11	1.93
Th		0.800		0.629		0.721			0.580		0.570	–		0.023		0.010	1.25	1.21
U		0.308		0.193		0.266			0.238		0.585	0.230		0.372		0.278	0.405	0.41
Traces[b]*—carbonate dissolution*																		
La	1.58	2.90	3.60	2.46	3.64	3.54	3.66	5.10	3.05	4.62	5.95	0.867	0.672	1.011	0.945	1.28	3.11	
Ce	2.91	5.09	7.47	4.30	2.34	2.38	2.44	2.87	4.00	3.56	2.92	0.196	0.149	0.247	0.201	0.307	6.81	
Pr	0.353	0.575	0.907	0.545	0.556	0.537	0.538	0.705	0.584	0.818	0.819	0.084	0.066	0.098	0.087	0.126	0.752	
Nd	1.36	2.40	3.47	2.18	2.47	2.18	2.50	3.07	2.47	3.73	3.67	0.337	0.311	0.486	0.412	0.553	3.060	
Sm	0.322	0.504	0.726	0.426	0.481	0.452	0.470	0.544	0.505	0.818	0.708	0.078	0.051	0.073	0.070	0.096	0.605	
Eu	0.064	0.115	0.173	0.096	0.125	0.121	0.117	0.145	0.126	0.237	0.191	0.017	0.015	0.021	0.018	0.028	0.138	
Gd	0.275	0.510	0.633	0.385	0.658	0.410	0.548	0.752	0.425	1.277	1.113	0.117	0.080	0.146	0.111	0.182	0.434	
Tb	0.051	0.070	0.096	0.064	0.100	0.092	0.091	0.106	0.099	0.169	0.160	0.023	0.013	0.016	0.014	0.027	0.106	
Dy	0.338	0.425	0.562	0.332	0.643	0.498	0.607	0.773	0.426	1.096	1.056	0.169	0.115	0.140	0.134	0.198	0.625	
Y	1.08	1.30	1.54	1.07	3.99	2.99	3.27	4.35	2.12	5.64	5.72	1.41	1.06	1.32	1.28	1.78	1.20	
Ho	0.062	0.095	0.110	0.073	0.154	0.106	0.154	0.201	0.090	0.245	0.253	0.041	0.029	0.039	0.037	0.043	0.104	
Er	0.159	0.270	0.284	0.197	0.464	0.381	0.439	0.528	0.346	0.704	0.709	0.132	0.107	0.126	0.107	0.146	0.254	
Tm	0.016	0.034	0.040	0.030	0.058	0.043	0.059	0.084	0.049	0.088	0.091	0.013	0.013	0.015	0.014	0.018	0.047	
Yb	0.120	0.223	0.289	0.192	0.402	0.298	0.350	0.488	0.220	0.504	0.553	0.128	0.099	0.095	0.088	0.093	0.245	
Lu	0.017	0.034	0.037	0.024	0.059	0.045	0.050	0.078	0.040	0.073	0.077	0.016	0.014	0.016	0.012	0.016	0.033	
Zr	0.111	0.109	0.125	0.097	0.145	0.120	0.129	0.123	0.105	–	–	0.115	0.151	0.092	0.090	0.033	0.146	
Hf	–	–	–	–	–	–	–	–	–	–	–	–	–	–	–	–	–	
Nb	–	–	–	–	–	–	–	–	–	–	–	–	–	–	–	–	–	
Ta	–	–	–	–	–	–	–	–	–	–	–	–	–	–	–	–	–	
Pb	1.93	3.05	1.13	0.804	0.606	0.545	0.426	0.983	0.701	0.890	0.895	0.139	0.175	0.199	0.245	0.162	0.648	
Th	0.194	0.610	0.536	0.535	0.299	0.462	0.252	0.364	0.452	0.352	0.230	–	–	–	–	–	0.661	
U	0.188	0.314	0.142	0.168	0.177	0.168	0.237	0.228	0.206	0.326	0.434	0.317	0.582	0.577	0.655	0.316	0.294	
$(La/Sm)_{SN}$	0.90	1.05	0.91	1.06	1.38	1.43	1.43	1.72	1.10	1.03	1.54	2.02	2.41	2.54	2.46	2.44	0.94	
$(Pr/Yb)_{SN}$	1.03	0.90	1.10	0.99	0.48	0.63	0.54	0.50	0.93	0.57	0.52	0.23	0.23	0.36	0.35	0.47	1.07	
$(Dy/Yb)_{SN}$	1.81	1.22	1.25	1.11	1.03	1.07	1.11	1.02	1.24	1.40	1.23	0.85	0.74	0.95	0.97	1.36	1.64	
(Ce*/Ce)	0.93	0.90	1.01	0.87	0.35	0.38	0.36	0.32	0.68	0.40	0.28	0.15	0.14	0.15	0.14	0.15	1.06	
(Pr*/Pr)	0.99	0.91	0.99	0.99	1.18	1.24	1.12	1.21	1.02	1.15	1.23	1.47	1.31	1.23	1.30	1.37	0.92	
Σ REE	7.6	13.2	18.4	11.3	12.1	11.1	12.0	15.4	12.4	17.9	18.3	2.2	1.7	2.5	2.3	3.1	16.3	

Major elements measured on whole rocks are expressed in wt.% oxide. Trace elements were measured on both whole rocks and carbonate fractions using two digestion methods. Concentrations are expressed in parts per million (ppm). Abbreviations: Microb., microbialites; Int. sed., internal sediment; Lat. sed., lateral sediment; Kim., Kimmeridgian; Oxf., Oxfordian.

[a] All major elements are recalculated to 100% volatile free; totals represent the sum of oxides and LOI in the original analysis.

[b] Reported ratios consider measurements obtained with carbonate dissolution. The subscript SN indicates that shale-normalized values were used. Ce and Pr anomalies were calculated using $(Ce/Ce^*)=Ce_{SN}/(La_{SN}^{2/3}\times Nd_{SN}^{1/3})$ after Grandjean-Lécuyer et al. (1993) and $(Pr/Pr^*)=Pr_{SN}/(0.5\times Ce_{SN}+0.5\times Nd_{SN})$, respectively.

and Lathuilière, 1991; Lathuilière et al., 2003; Olivier et al., 2004a) and Plettenberg locations (Olivier et al., 2004b).

At the Chay Peninsula (Charente-Maritime, France), four samples (Cp1–4) were collected from Lower Kimmeridgian coral-microbialite reefs. These bioconstructions are situated on a mixed carbonate-siliciclastic and low- to moderate-energy ramp, on the eastern Atlantic Ocean margin (Fig. 1). Coral-microbialite bioherms developed laterally to limestone deposits (Table 1). In these bioconstructions, microbialites are two-layered and form up to 70% of the reef volume. The first microbialite layer displays a thrombolitic (or locally a leioitic) fabric. This relatively thin (<1 cm) layer is directly observed on the coral surface. The second microbialite layer can reach 8 cm thick and generally shows a thrombolitic fabric. Within the bioconstruction, samples Cp1–3 correspond to mammilated microbialites of bioherm flanks or undersides (Fig. 2). Sample Cp4 is a pseudostalactitic microbialite observed at the roof of intra-reef cavities. All microbialites were collected in the second centimeter-scale layer.

Coral-microbialite reefs of Pagny-sur-Meuse (Lorraine, France) are located on the eastern margin of the Paris Basin (Fig. 1). During the Middle to Upper Oxfordian interval, these bioconstructions developed on an isolated platform on the northeastern margin of the Tethys Ocean (Carpentier, 2004). Five samples (Pm1–5) come from a coral-microbialite reef level located in a pure carbonate lagoon. This reef level consists of wide bioherms (about 100 m large and 15 m thick), which contain a moderate amount of microbialites (up to 16% of the reef volume). One sample (Pm6) was collected in a reef level that developed in a mixed carbonate-siliciclastic lagoon. These bioconstructions, made of a high amount of microbialites (up to 50% of the reef volume), developed laterally to limestone deposits (Table 1), above and below marly levels. Similarly to the Chay Peninsula, microbialites of Pagny-sur-Meuse are two-layered and generally show a thrombolitic fabric. Samples Pm1–2 and Pm6 were collected from mammilated microbialites of bioherm undersides, Pm3–4 from pseudostalactitic microbialites and Pm5 from intra-reef sediments. All microbialite samples correspond to the second microbialite layer (Fig. 2).

Samples from Plettenberg (Upper Oxfordian, southern Germany) were collected from sponge-microbialite bioherms of the Swabian Alb (Fig. 1). These bioconstructions developed within carbonate-dominated deep shelf to epicontinental basin settings on the northeastern margin of the Tethys Ocean (Meyer and Schmidt-Kaler, 1990; Pittet and Strasser, 1998). In these sponge-microbialite bioherms, microbialite crusts are situated on the upper surface of tube- or dish-shaped sponges and form up to 30% of the reef volume. Sponge-microbialite bioherms show a centimeter-scale and well-discernable multi-stage growth of microbialites made of three main successive layers (Fig. 2). The first microbialite layer (sample Pt1) is relatively thin (<2 cm) and shows a leolitic or a thrombolitic fabric. The second microbialite layer (samples Pt2 and Pt3) corresponds to thick (up to 10 cm high) thrombolitic columns. The last and third microbialite layer (samples Pt4 and Pt5), characterised by a stromatolitic fabric, is progressively buried beneath carbonate-dominated detrital sediments. Sample Pt6 corresponds to intra-reef sediments and Pt7 was collected in a limestone bed laterally to a sponge-microbialite bioherm.

2.2. Analytical methods

In coral- or sponge-microbialite bioconstructions, centimeter-scale microbialites developed on a coral or sponge support. These microbial crusts are recognizable by their non-gravitational growth forms and by a darker colour than sediments. Nevertheless, the sampling of microbialites is made more difficult by the heterogeneity of the encrustation that also contains millimeter- to centimeter-scale zones of sediments and diverse millimeter-scale organisms such as foraminifers, annelids, bryozoans and calcareous sponges. In order to analyse only microbialite portions, sampling was done from polished slabs under binocular lens. The petrological examination of thin sections showed that the detrital carbonate- and siliciclastic-fine sediments were absent in most of microbialite samples. Only the third stromatolitic layer observed in sponge bioherms contains rare siliciclastic grains into micrometer- to millimeter-scale horizons made of carbonate particles.

Each sample was crushed in an agate mortar to obtain fine powders. Different geochemical analyses (major elements, trace elements and Sm–Nd isotopes) were performed on different aliquots. Major elements were measured on whole rock by X-ray fluorescence (XRF spectrometer Phillips PW1404) at the University of Lyon. Analytical uncertainty ranges from 1% to 2% for major elements. Trace elements were measured using two different digestion methods. In the first one called “whole rock”, bulk samples were dissolved on hot plate (130 °C for 48 h) in a mixture of concentrated HF-HNO_3 within sealed PFA Savillex beakers. In the second one called “carbonate selective dissolution”, only the pure carbonate fraction was dissolved by acetic acid. With acetic acid, the carbonate selective

dissolution is ensured, in contrast to methods using nitric or chlorydric acids, since REE contained in siliciclastic grains are partly dissolved. This method was inspired from Boyle and Keigwin (1985) procedure applied on foraminifers and modified by Pichat (2001). The samples were rinsed three times using distilled water, ethanol and distilled water successively. Once the residual part dried, 1 M acetic acid was added and the samples were heated for a minimum of 12 H at 130 °C. After cooling, the samples were centrifuged and the supernatant solution (carbonate part) was conserved. This procedure was repeated twice. Finally, in order to reduce the amount of organic matter, the samples (i.e. mixing of different carbonate fractions) were dissolved three times with a solution of 7 M HCl–0.1% H_2O_2. Each sample was dissolved in HNO_3 0.5 M and spiked with 10 ppb of In and Bi in order to measure trace concentrations by ICPMS Plasma Quad (VG Elemental) at the Ecole Normale Supérieure of Lyon. Analyse of pure elemental solution lead to monitor the oxide levels and has been used to calculate precise interference correction. In order to validate our measurements, the standard BHVO-1 was dissolved (HF-NO_3) and measured in the same conditions. Determined concentrations are in perfect agreement with recommended values for this standard published in Govindaraju (1994, Table 2). Analytical uncertainty is about 10% for trace elements. Elements not reported in Table 2 could not be measured due to concentrations under detection limits. Isotope analyses (chemistry and mass spectrometry) were realised at the Department of Terrestrial Magnetism (Carnegie Institution of Washington). Sm–Nd isotope chemistry has been applied for 12 samples coming from two locations, Plettenberg and Pagny-sur-Meuse. The two samples Pm7 and Pm8 from Pagny-sur-Meuse have not been analysed for trace elements, but are lithologically and stratigraphically similar to Pm1 and Pm5 samples, respectively. Before the dissolution procedure, a mixed ^{149}Sm–^{150}Nd spike solution was added to samples to determine concentrations of these elements by isotope dilution. Sm and Nd were separated using two ion-exchange columns. First of all, REE was separated using the transuranic-element specific resin (TRU.Spec) and a modified procedure after Pin and Zalduegui (1997). Sm and Nd fractions were finally separated in 0.2 M α-hydroxyisobutyric acid with a pH equal to 4.7. Total procedural blanks measured were 13 and 60 pg for Sm and Nd, respectively. Nd concentrations and isotopic compositions were determined using the new generation thermal-ionization mass spectrometer (Triton). Mass 147 was monitoring to correct Sm isobaric interference on mass 144.

Table 3
Sm–Nd isotope data of Pagny-sur-Meuse and Plettenberg samples

Sample	[Sm][a], ppm	[Nd][a], ppm	$^{147}Sm/^{144}Nd$	$^{143}Nd/^{144}Nd$, $\pm 2\sigma/\sqrt{n}$ [b]	$\varepsilon_{Nd(T)}$ [c]
Pm1	0.0889	0.502	0.1072	0.512219±13	−6.4
Pm2	0.0684	0.381	0.1085	0.512213±3	−6.5
Pm3	0.0884	0.510	0.1049	0.512243±8	−5.9
Pm5	0.110	0.634	0.1045	0.512247±5	−5.8
Pm7	0.0956	0.545	0.1061	0.512243±6	−5.9
Pm8	0.0861	0.488	0.1066	0.512232±5	−6.1
Pm6	0.763	3.98	0.1159	0.512041±3	−10.0
Pt1	0.554	3.04	0.1101	0.512153±3	−7.7
Pt2	0.609	3.36	0.1095	0.512147±3	−7.9
Pt3	0.475	2.60	0.1103	0.512169±3	−7.4
Pt5	0.508	2.71	0.1133	0.512103±6	−8.8
Pt6	0.735	3.92	0.1134	0.512183±3	−7.2

[a] Sm and Nd concentrations were determined by isotope dilution.
[b] Uncertainties reported on Nd measured isotope ratios are in-run $2\sigma/\sqrt{n}$ analytical errors in last decimal place, where n is the number of measured isotopic ratios. $^{143}Nd/^{144}Nd$ was normalized for mass fractionation to $^{146}Nd/^{144}Nd=0.7219$.
[c] Initial ε_{Nd} values were calculated at age $T=156$ Ma using $\lambda^{147}Sm=6.54\times10^{-12}$ a^{-1} and the following modern CHUR values: $^{143}Nd/^{144}Nd=0.512638$ and $^{147}Sm/^{144}Nd=0.1967$. $\varepsilon_{Nd(T)}=[(^{143}Nd/^{144}Nd)_{sample,T}/(^{143}Nd/^{144}Nd)_{CHUR,T}-1)\times10^4]$.

Isotopic ratios are corrected of mass fractionation using $^{146}Nd/^{144}Nd=0.7219$. Internal errors ($2\sigma_{mean}$) are reported in Table 3 and the external reproducibility was obtained by repeated measurements of La Jolla Nd standard (0.511846±3). Sm concentrations were determined by multiple-collector inductively coupled plasma mass spectrometer (VG Plasma 54).

3. Results and discussion

3.1. Microbialite and sediment chemistry

3.1.1. Major elements

All microbialites and sediments analysed are carbonate rocks composed of 85% to 99% of CaO (Table 2). Samples from Pagny-sur-Meuse (Pm1–5) are particularly rich in CaO (>98%) with SiO_2 content lower than 0.2%. Pm6, collected in the same location, but in a different reef level, has a higher amount of siliciclastic material ($SiO_2=7\%$ and $CaO=88\%$). Microbialite samples of other localities (Chay Peninsula and Plettenberg) show relatively similar compositions: SiO_2 between 3% and 5.5%, Al_2O_3 in the range of 1% to 2% and MgO lower than 1.5%. The intra-reef sediments of Plettenberg (Pt6) are particularly rich in SiO_2 (8.7%) and Al_2O_3 (3.2%). Sediments collected in limestone levels laterally to sponge- and coral-microbialite reefs (Pt7 and Pm5, respectively) have a composition close to those of contemporaneous microbialites (Table 2).

3.1.2. Trace elements

Trace element concentrations of microbialites and associated sediments are relatively low and never exceed few micrograms per gram or parts per million (ppm) for both digestion methods (Table 2). Analyses realised on bulk samples show higher concentrations for most of trace elements, notably for carbonate samples enriched in siliciclastic material. Lithophile elements characterised by short residence times in seawater, such as Zr and Th, show higher concentrations for bulk dissolution, whereas their abundances strongly decrease for analyses on carbonate fractions. Highly incompatible elements (i.e. concentrated in crustal material), such as light rare earth elements (LREE), are clearly more abundant when the siliciclastic part is dissolved. However, the LREE budget is dominantly contained in the carbonate fraction. For example, La content increases of a factor lower than 1.5 for bulk sample measurements relative to carbonate analysis. The influence of terrigenous material on the REE budget is illustrated in Fig. 3. SiO_2 is strongly correlated to Al_2O_3 content (Fig. 3a) and these oxides are directly related to the REE content, expressed here by the sum of REE (Fig. 3b). This positive correlation is observed considering REE contents measured on either bulk samples or carbonate fraction only. Elements like Hf, Nb and Ta can be measured using bulk rock dissolution but are below the ICPMS detection limits for carbonate fractions.

Samples from different localities are represented using shale-normalized (subscript SN) carbonate-fraction REE patterns (Fig. 4), considering the mean composition of North American, European and Russian shales from Haskin and Haskin (1966), Piper (1974) and Byrne and Sholkovitz (1996). Common elemental ratios, used in this work to describe REE patterns, are reported in Table 2. Samples from the Chay Peninsula have relatively similar REE flat patterns [$(Pr/Yb)_{SN}=0.9–1.1$] with a slight depletion in heavy REE (HREE) compared to the middle REE (MREE) [$(Dy/Yb)_{SN}=1.1–1.8$; Fig. 4a]. Ce anomalies, calculated after Grandjean-Lécuyer et al. (1993) equation $(Ce/Ce^*)=Ce_{SN}/(La_{SN}^{2/3}\times Nd_{SN}^{1/3})$, are very close to zero (0.9–1.0). The REE patterns of Plettenberg samples are depleted in LREE related to HREE [$(Pr/Yb)_{SN}<0.9$; Fig. 4b] and HREE are sensibly depleted [$(Dy/Yb)_{SN}=1–1.4$]. Ce anomalies are negative and comprised between 0.3 and 0.6. Different types of microbialites, intra-reef (Pt6) and lateral (Pt7) sediments show very comparable REE patterns. At Pagny-sur-Meuse, microbialites and intra-reef sediments sampled in pure carbonate setting have the lowest REE concentrations (≈0.01 times the shale concentration; Fig. 4c). Microbialites are characterised by significant HREE enrichments [$(Pr/Yb)_{SN}<0.5$] and very strong negative Ce anomalies [$(Ce/Ce^*)=0.15$]. The microbialite sample collected in the mixed carbonate-siliciclastic environment (Pm6) has

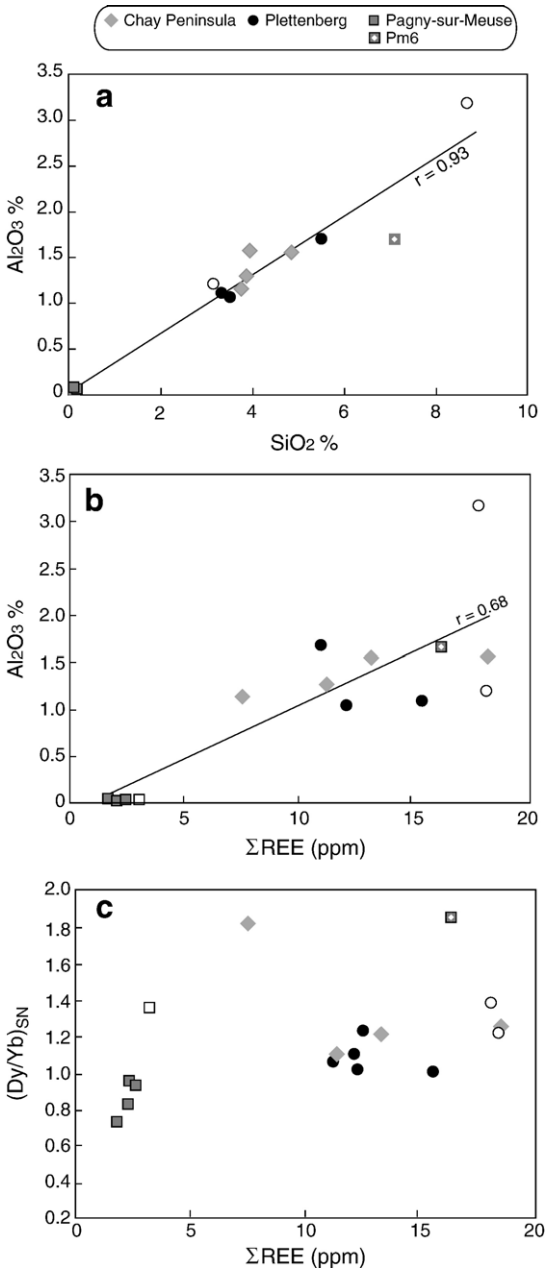

Fig. 3. Binary diagrams illustrating variations of trace concentrations relative to the amount of siliciclastic material (SiO_2 and Al_2O_3). Major elements expressed in wt.% oxide were measured on bulk samples, whereas REE correspond to measurements on carbonate fractions. (a) Al_2O_3 vs. SiO_2, (b) Al_2O_3 vs. ∑REE, (c) $(Dy/Yb)_{SN}$ vs. ∑REE. Sediments are represented by open symbols. See text for more explanations.

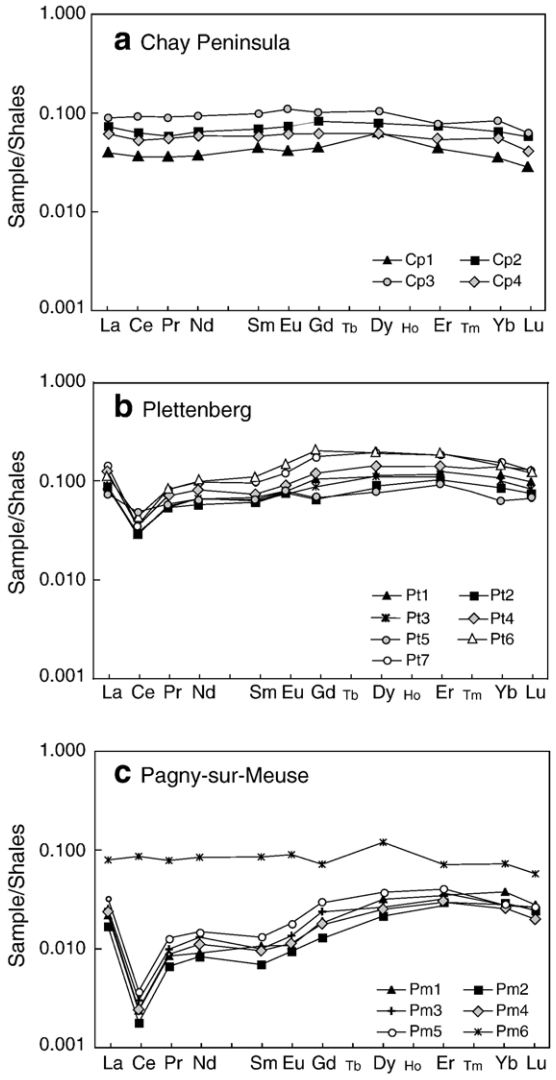

Fig. 4. Shale-normalized REE patterns for the Chay Peninsula (a), Plettenberg (b) and Pagny-sur-Meuse (c) samples measured on carbonate fractions. The average of North American, European and Russian shale composites (Haskin and Haskin, 1966; Piper, 1974; Byrne and Sholkovitz, 1996) is used for normalization. Lateral and intra-reef sediments are represented by open symbols.

10 times higher REE concentrations and a more flat pattern [$(Pr/Yb)_{SN}=1.1$] with a depletion in HREE [$(Dy/Yb)_{SN}=1.6$]. Furthermore, Pm6 does not show a Ce anomaly [$(Ce/Ce^*)=1.09$]. The pattern of this specific sample is close to those of the Chay Peninsula microbialites (Cp1–4). The presence of terrigenous material and its effects on REE budget for samples from these three locations is illustrated in Fig. 3b and c. Fig. 3c shows a positive correlation between the $(Dy/Yb)_{SN}$ ratio with the sum of REE. The enrichment in HREE relative to MREE is well marked for Pagny-sur-Meuse samples (expect Pm6), whereas samples from other locations, characterised by higher aluminium and silicon contents, tend to have more flat shale-like REE patterns.

3.1.3. Neodymium isotopes

Isotopic ratios and Sm–Nd concentrations determined by isotopic dilution are presented in Table 3. $^{143}Nd/^{144}Nd$ ratios were corrected for a microbial carbonate age formation of 156 Ma (i.e. approximate age of microbialite samples according to the timescale after Gradstein et al., 1994). Considering the initial isotopic ratios, three groups of samples are differentiated. All Pagny-sur-Meuse microbialites have similar ε_{143Nd} (-6.1 ± 0.6, 2σ). Slightly more negative values characterise samples from Plettenberg (-7.8 ± 1.2). This dispersion is strongly reduced (-7.7 ± 0.4) by leaving out the two extreme ε_{143Nd} corresponding to sample Pt5, collected in the third stromatolitic layer, and lateral sediment (Pt6). Pm6 has the most negative ε_{143Nd} (-10.1). The $^{147}Sm/^{144}Nd$ ratios fall in a remarkably narrow range (0.1045–0.1159) with a mean value equal to 0.1092 ± 0.0072 ($\pm2\sigma$).

3.2. Microbialites and seawater REE chemistry

3.2.1. Microbialites as proxy in geochemical seawater reconstructions

Several features argue for a record of the original seawater REE chemistry in microbialites. These carbonates result of a biologically induced precipitation within biofilms or algal mats (Riding, 2000). Webb and Kamber (2000) demonstrated that REE are incorporated in high proportion and without biological fractionation in modern microbialites. Works on carbon and oxygen isotopes confirmed that ancient microbialites precipitate at equilibrium with seawater (e.g. Keupp et al., 1993; Schmid, 1996; Camoin et al., 1999). Moreover, REE concentrations in carbonates tend to be relatively stable through diagenesis (Banner et al., 1988), and no post-depositional modifications in REE signature of Paleozoic and Precambrian microbialites have been identified (Kamber and Webb, 2001; Van Kranendonk et al., 2003; Nothdurft et al., 2004).

Analysed microbialites encrusted a previous skeletal framework made of sponges or corals, suggesting growth well-above the sea floor (Fig. 2). Only microbialites of stromatolitic fabric, collected in sponge bioherms of Plettenberg, grew in contact with sea-floor sediments. The fixation and overgrowth of various encrusters (e.g. calcareous sponges and bryozoans) on microbialite surfaces indicate a rapid lithification (Dromart et al., 1994). These observations argue for a record

of microbialite REE signature before being covered by sediments, reducing thus an eventual chemical modification by porewaters. Petrographically, all studied microbialites seem not affected by late diagenetic processes, like intense sparitisation or recrystallization. Microbialites are made of micritic calcite, which can be dense, clotted or locally peloidal, with only minor portions of spar cements. Among geochemical tracers, trace elements and isotopes can aid in the detection of diagenetic alteration. An influence of diagenetic fluids derived from meteoritic sources lead to enhance the Mn content (Brand and Veizer, 1980). Analysed microbialites have relatively low Mn and U contents lower to 300 ppm and 0.5 ppm, respectively. The fact that $^{143}Nd/^{144}Nd$ ratios measured in these microbialites (ε_{143Nd} between −5.9 and −8.8) are in the range of previous determinations for the Tethys seawater at 150 Ma (e.g. Stille et al., 1996) argues for a non-perturbation of REE during post-depositional events. Only Pm6, with a Mn content of 400 ppm and a ε_{143Nd} of −10.0, differs from other measurements. Such different chemical composition can reflect post-depositional modifications but also can be linked to a higher terrigenous contamination. Geochemical arguments in favor of the second scenario will be discussed in detail in the next section. According to this set of evidences, studied microbialites are considered to be not significantly diagenetically altered and thus can be used to examine ancient seawater chemistry.

Lateral and intra-reef sediments have been analysed for Pagny-sur-Meuse and Plettenberg localities. Sediments significantly differ from microbialites by an increase of ∑REE and $(Dy/Yb)_{SN}$ ratio (Fig. 3c). Considering that detrital carbonate sediments are made of auto- and allochthonous components, a higher heterogeneity in their chemical composition is expected. For example, the limestone beds located laterally to the sponge-microbialite bioherms of Plettenberg have a large proportion of carbonate mud exported from shallow and proximal platform (Pittet and Strasser, 1998; Pittet and Mattioli, 2002). With a formation in positions nearer to siliciclastic sources, this exported carbonate mud can provide to lateral and intra-reef sediments a higher terrigenous contamination than microbialites. Therefore, chemical composition of microbialites alone will be considered in the following discussion to reconstruct the Upper Jurassic seawater REE chemistry.

3.2.2. Upper Jurassic seawater REE chemistry

In the current representation of shale-normalized patterns, the modern seawater is characterised by: La enrichment relative to heavier neighbouring lanthanides, positive Gd anomaly, strong negative Ce anomaly and HREE enrichment relative to MREE and LREE (e.g. Byrne and Sholkovitz, 1996). Two processes are important for incorporating REE into sediments, the adsorption from seawater and the inclusion of clastic material (Murray et al., 1991). Siliciclastic material present in carbonate or phosphate sediments plays an important role in the REE budget and is able to mask the seawater signature (Piper, 1974; Grandjean et al., 1987; Murray et al., 1990). In proximal settings, the incorporation of siliciclastic particles is the prevalent process because terrigenous input can be relatively important and high accumulation rates reduce the time during which the sediment is exposed to the surrounding water (Davies and Pickering, 1999). Since the studied carbonates were collected in proximal settings and in different depositional environments (pure carbonate to mixed carbonate-siliciclastic), the issue of terrigenous contamination need to be addressed.

Pagny-sur-Meuse microbialites (Pm1–4) are devoid of terrigenous contamination ($SiO_2 < 0.2\%$) and their shale-normalized REE patterns present all the chemical characteristics of the modern seawater (Fig. 4c). These samples are notably characterised by enrichment in HREE relative to MREE and a net deficit in Ce. At ambient oceanic condition, Ce is oxidized into insoluble Ce^{4+}, which is quickly subtracted from the seawater by preferential adsorption on particle surfaces (Elderfield, 1988). On the other hand, microbialites collected in carbonate-dominated (Plettenberg) and mixed carbonate-siliciclastic (Chay Peninsula and Pm6) settings are not free from continental contamination. In order to appreciate the terrigenous contamination part in REE compositions of microbialites, a binary mixing model has been done (Fig. 5a). The first end-member, assimilated to the Upper Jurassic seawater composition, corresponds to the average of Pagny-sur-Meuse microbialite (Pm1–5) compositions. The second end-member is a detrital pole of shale composition (Haskin and Haskin, 1966; Piper, 1974; Byrne and Sholkovitz, 1996). This calculation shows that a very low amount of terrigenous material in the mixing (>1% and equivalent to $SiO_2 > 0.7\%$) is sufficient to mask the seawater REE pattern in significantly reducing the negative Ce anomaly and the HREE enrichment relative to LREE. Microbialites from mixed carbonate-siliciclastic settings (Chay Peninsula and Pm6) are located very close to the shale end-member. Although these microbialites present very flat REE patterns [$(Pr/Yb)_{SN} = 0.9–1.1$], few samples (Cp1–2 and 4) have preserved a low negative Ce anomalies [$(Ce/Ce^*) = 0.87–0.93$]. The Ce anomalies reported in Table 2 were calculated using the two neighbouring elements, La and Nd. However, considering Ce

anomaly values may reflect anomalous La abundances in modern seawater, Bau and Dulski (1996) evaluated Ce anomalies with the (Pr/Pr*) ratio [$Pr_{SN}/(0.5Ce_{SN}+0.5Nd_{SN})$]. Because neither Pr_{SN} nor Nd_{SN} anomalies exist, (Pr/Pr*) ratios higher than 1 emphasize negative Ce anomalies. Samples, with apparent negative Ce anomalies but with a ratio (Pr/Pr*) ≈ 1, have in fact positive La anomalies. The graph (Pr/Pr*) vs. (Ce/Ce*) shows that Ce content deficits calculated for the Chay Peninsula microbialites (Cp1–2 and 4) reflect La enrichments (Fig. 5b). Microbialites from carbonate-dominated environments (Plettenberg) show real negative Ce anomalies in the range of modern seawater values. One sample, Pt5, is slightly remote from other samples of Plettenberg, with a flat REE pattern [$(Pr/Yb)_{SN}=0.9$] and no negative Ce anomaly (Fig. 5a and b). Pt5 has a stromatolitic fabric made of an alternation of microbial layers with detrital deposits. This stromatolitic crust represents the final stage of microbialite development on the upper face of siliceous sponges before being definitively covered by sediments (Fig. 2). The REE composition of Pt5 could have been modified by the presence of Ce-rich porewaters (Sholkovitz et al., 1996). However, since another stromatolitic sample (Pt4) displays very close chemical characteristics than other microbialites of Plettenberg, the influence of porewater is probably limited. This heterogeneity in the REE composition of stromatolite samples is most likely due to different amounts of terrigenous material and detrital carbonate trapped within this type of microbialites.

Microbialites from carbonate-dominated (Plettenberg) and mixed carbonate-siliciclastic (Chay Peninsula and Pm6) environments recorded different REE patterns for an equivalent range of terrigenous contamination (SiO_2 3–9% and Al_2O_3 1.1–1.7%; Figs. 3, 4 and 5). The silica content measured on bulk rock is directly dependent of the amount of particles accumulated during the microbialite growth. The two prevalent mineral phases, quartz and clay minerals, have very different affinities for REE. Clay minerals have very high partition coefficients for these elements whereas quartz particles contain almost no REE. The carbonate selective dissolution of microbialites with acetic acid solution can

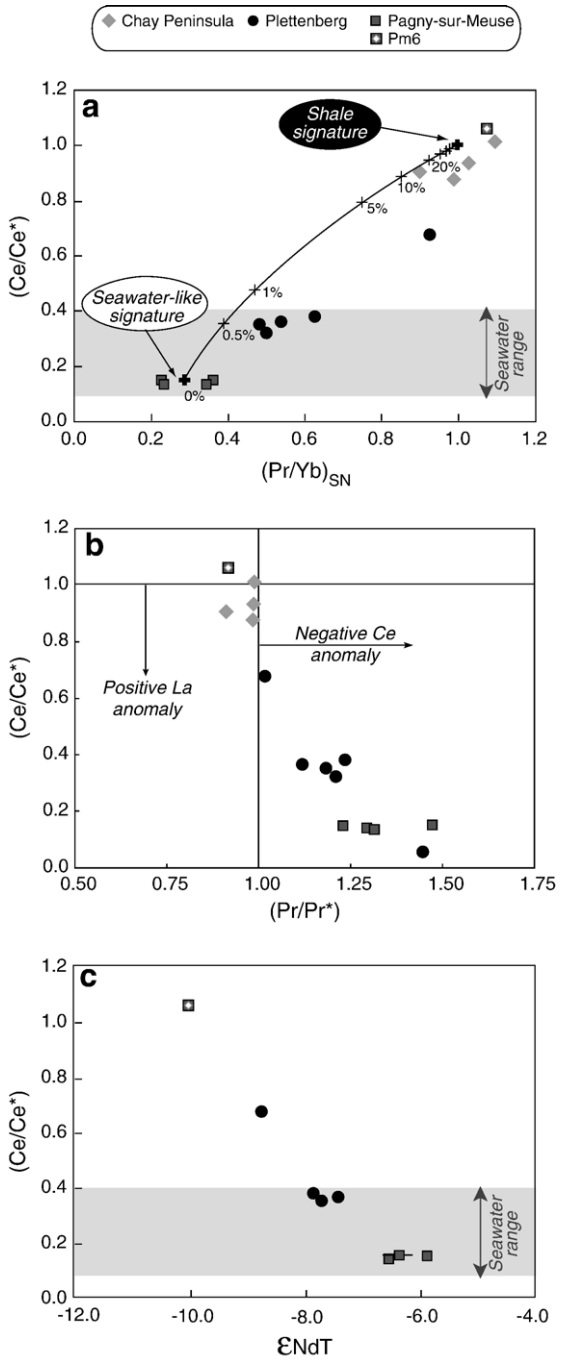

Fig. 5. Series of diagrams focussing on Ce anomalies (Ce/Ce*) measured in microbialites collected in different paleoenvironments. (a) (Ce/Ce*) vs. $(Pr/Yb)_{SN}$ showing the evolution of Ce anomaly in relation to terrigenous content. The diminution of Ce anomaly correlated to the increase of $(Pr/Yb)_{SN}$ ratio can be induced by a higher terrigenous contribution. The mixing curve between a pure carbonate end-member, average of Pagny-sur-Meuse microbialites (Pm1–4) and a detrital end-member of shale composition is traced. A very low contribution of detrital component (>1% of the mixing) is enough to significantly mask the seawater signature. (b) Binary diagram (Ce/Ce*) vs. (Pr/Pr*) allowing the discrimination between Ce and La anomalies (after Bau and Dulski, 1996). (c) (Ce/Ce*) vs. ε_{Nd} corresponding to the initial $^{143}Nd/^{144}Nd$ calculated for 156 My. The strong negative correlation argues for a lost of Ce anomaly by adding siliciclastic material. Microbialites with Ce anomalies comprised in seawater range value (grey field) have also ε_{Nd} perfectly consistent with values determined for the Tethys seawater around 150 My. See text for more precise explanations.

cause the release of metallic cations from the clays. However, low REE contents and very similar shale-normalized REE patterns, obtained from bulk or carbonate selective dissolutions argue against a significant contribution of clay minerals on the REE budget for analysed microbialites. An equivalent clay contribution in microbialites from carbonate-dominated and mixed carbonate-siliciclastic settings is also supported by similar Al_2O_3 contents and a strong positive correlation between Al_2O_3 and SiO_2 (Fig. 3a). A more probable explanation for similar SiO_2 contents and different REE patterns is that siliciclastic particles trapped by microbialites do not reflect the amount present in the water column. In some modern shallow platform settings, siliciclastic material can dominantly be in transit towards more distal environments (e.g. Woolfe and Larcombe, 1998). Underestimation of the terrigenous contamination in mixed carbonate-siliciclastic settings (Chay Peninsula and Pm6) is effectively expected in the binary mixing model (Fig. 5a). Mixing calculation suggests a terrigenous contamination higher than 10% (equivalent to $SiO_2 > 6\%$) for the Chay Peninsula and Pagny-sur-Meuse (Pm6) microbialites, whereas measured SiO_2 are lower than 5%.

These results show that microbialites selected in a pure carbonate setting (Pagny-sur-Meuse) clearly reflect the original REE seawater signature. Although microbialites from carbonate-dominated settings (Plettenberg) display chemical characteristics close to modern seawater (e.g. negative Ce anomalies), their REE composition is slightly affected by a continental contamination. Nd isotopes are consistent with these conclusions since microbialites from pure carbonate settings have very uniform $^{143}Nd/^{144}Nd$ ratios with initial $\varepsilon_{143Nd(T)} = -6 \pm 0.6$ (2σ), which is similar to the Tethys seawater range values obtained on same age (~150 Ma) marine phosphate (fish remains), fossil debris and Mn ores (Shaw and Wasserburg, 1985; Grandjean et al., 1987; Stille et al., 1989, 1996). The good correlation between the Ce anomalies and $\varepsilon_{143Nd(T)}$ confirms various degree of terrigenous contamination for microbialites according to the depositional setting (Fig. 5c). Microbialites from carbonate-dominated [Plettenberg; $\varepsilon_{143Nd(T)}$ (−7.5 to −8.8)] and mixed carbonate-siliciclastic [Pm6; $\varepsilon_{143Nd(T)} = -10 \pm 0.6$ (2σ)] environments reflect a contamination by a crustal material characterised by a signature that is particularly unradiogenic.

3.2.3. Composition of seawater over geological time

This study focuses on seawater chemistry recorded in Upper Jurassic microbialites and presents the first REE data recorded by this carbonate-type sediment during the Mesozoic. Microbialites collected in Upper Jurassic coral and sponge reefs developed before the progressive radiation of the calcareous plankton during the Cretaceous times (Roth, 1986). Removal of $CaCO_3$ by coccolithophore algae and globigerine foraminifers significantly affected the seawater chemistry in reducing the saturation state, and consequently was probably responsible of the microbial carbonate decline after the Jurassic (Riding and Liang, 2005a,b). Different works based on phosphate sediments also suggest that ancient seawater REE chemistry was significantly different before Upper Cretaceous times and was characterised by a net HREE depletion (McArthur and Walsh, 1984; Grandjean et al., 1987, 1988; Grandjean-Lécuyer et al., 1993; Ilyin, 1998; Picard et al., 2002; Lécuyer et al., 2004). These authors evoke change of the planktonic biomass may have affected the HREE fractionation in modifying the scavenging mechanism of REE in the water column. However, the identification of post-depositional modifications of phosphate REE signatures by diagenetic processes questions the use of phosphate sediments for REE seawater reconstructions (Reynard et al., 1999; Shields and Stille, 2001; Shields and Webb, 2004). Upper Jurassic microbialites collected in pure carbonate and shallow (<30 m) settings of Pagny-sur-Meuse show a net HREE enrichment with $(Dy/Yb)_{SN}$ ratios comprised between 0.74 and 0.97 and a negative Ce anomaly (0.14–0.15) similar to modern shallow seawater (Piepgras and Jacobsen, 1992; Zhang and Nozaki, 1996; Alibo and Nozaki, 1999). Very close microbialite REE patterns obtained in deep shelf to epicontinental basin (70–150 m) settings (Plettenberg) argue for homogeneous REE seawater chemistry at the scale of the northwestern Tethys margin. Based on our data and those from the literature, microbialites from the Archaean to the present time present close shale-normalized patterns but are also very similar to the modern seawater (Fig. 6). Considering that microbialites record REE seawater composition through time, no major modifications of the REE seawater chemistry would have occurred, especially for Phanerozoic times. With relatively similar REE patterns, which may differ for example in La or Ce anomalies, microbialites are thus robust proxies for ancient seawater chemistry reconstructions (see also Kamber and Webb, 2001; Nothdurft et al., 2004; Kamber et al., 2004; Shields and Webb, 2004).

3.3. Depositional environment of microbialites

The predominance of abundant quantities of microbialites in Upper Jurassic reef ecosystems implies ambient seawater favourable to carbonate non-

enzymatic biomineralization. Although microbial induction of carbonate precipitation results from various and complex microbial heterotrophic and autotrophic processes, the saturation state with respect to carbonate minerals is frequently related to carbonate alkalinity and/or pH increases (cf. Castanier et al., 1999; Riding, 2000; Webb, 2001). Alkalinity is thus evoked to favour the microbialite formation in cavities of modern coral reef (Reitner, 1993) and in some lake waters (Thompson et al., 1990; Arp et al., 1996; Kempe et al., 1996). Past oceans, so-called "soda-oceans", also could be characterised by higher alkalinity, explaining the large amount of microbial carbonates in Precambrian times (Kempe and Degens, 1985; Arp et al., 2001). The strong pH dependence of the Ce concentrations also complicates the use of Ce anomalies as proxy for oxic and anoxic seawaters (de Baar et al., 1985; Cantrell and Byrne, 1987; Byrne and Kim, 1993). In alkaline and high-pH waters of Lake Van (pH=9), Möller and Bau (1993) explained the net positive Ce anomalies by the good stabilization of polycarbonate-Ce^{4+} complexes in solution. Abundant inorganic ions CO_3^{2-} and OH^- present in rivers or seawaters with high pH form stronger complexes with HREE than LREE, resulting in HREE enriched shale-normalized patterns (Goldstein and Jacobsen, 1988; Byrne and Kim, 1990). Absence of positive Ce anomalies, as well as strongly enriched HREE patterns in analysed microbialites suggest that ambient seawater, were characterised by neither a high alkalinity nor a pH higher than 8.2, the value of modern seawater. These arguments support the control of Ce anomalies in microbialites by REDOX conditions, allowing discussion on depositional environments for the different studied localities.

In the pure carbonate setting of Pagny-sur-Meuse, coral associations suggest oligotrophic conditions during the edification of the coral framework (Fig. 7a; Olivier et al., 2004a). Observed directly on the coral reef surface, microbialitie crusts (Pm1–5) show a seawater-like REE patterns with strong negative Ce anomalies. This suggests a well-oxygenated water column devoid of terrigenous materials during the microbialite formation. In such environment, the microbialite development is not linked to an increase of terrigenous input, but rather, to the release of nutrients from sediments and porewaters following important storm events (cf. Olivier et al., 2004a). However, preferential releases of LREE and Ce from sediments in porewaters should remove the Ce anomaly and flatten the patterns. Seawater-like REE patterns suggest that the release of lanthanides from sediments were probably too limited in time to affect the entire water column and thus being recorded in microbialites. On the other hand, the coral community disturbance, coupled to a temporarily rise of nutrients release from the sediments after a major tempest event, is sufficient to allow a benthic microbial bloom. After reaching a critical point, benthic microbial communities could also prevent coral recovery (McCook, 2001), permitting the microbialite formation.

In more distal settings of deep shelf to epicontinental basin, formation of microbialites at the surface of sponge bioherms is frequently assumed to have occurred in anoxic–dysoxic seawaters (Leinfelder et al., 1993, 1994, 1996; Schmid, 1996; Schmid et al., 2001; Leinfelder, 2001). Despite a certain degree of terrigenous contamination, Ce anomalies [(Ce/Ce*)=0.3–0.7] reported in Plettenberg samples evoke relatively well-oxygenated seawaters during formation of microbialites (Fig. 7b). Nutrients associated with a relatively moderate terrigenous influx probably controlled microbialite development on the primary sponge framework (Olivier et al., 2004b).

In mixed carbonate-siliciclastic settings of Pagny-sur-Meuse (Pm6) and the Chay Peninsula, coral associations point out mesotrophic conditions (Olivier, 2004). The upwelling of deep-waters rich in nutrients and possibly poorly oxygenated has been suggested to explain formation of abundant microbialites (up to 70% of the reef volume) on coral surface of the Chay Peninsula reefs (Leinfelder, 2001). Normalized shale-like REE patterns of microbialites from these mixed carbonate-siliciclastic settings (Chay Peninsula and Pm6) clearly show the contribution of terrigenous material. The small amount of siliciclastics is sufficient to mask the REDOX conditions occurring in the water column during the formation of microbialites (Fig. 7a).

Therefore, this study contends that Upper Jurassic microbialites were able to form in well-oxygenated (and possibly in dysoxic?) seawaters. Shale-normalized REE patterns also suggest normal pH and alkalinity in the water column during the microbialite formation at the surface of studied coral and sponge reefs. The carbonate precipitation probably occurred directly within the biofilm, in local microenvironments, favoured by biological effects on saturation states and on nucleation (e.g. Webb, 2001; Nothdurft et al., 2005). In all cases, their development is consistent with an increase in the nutrient content (Olivier et al., 2004a,b). Higher trophic conditions in ambient seawater probably allowed blooms of benthic microbial communities, which finally covered coral and sponge frameworks, such as it is observed in some

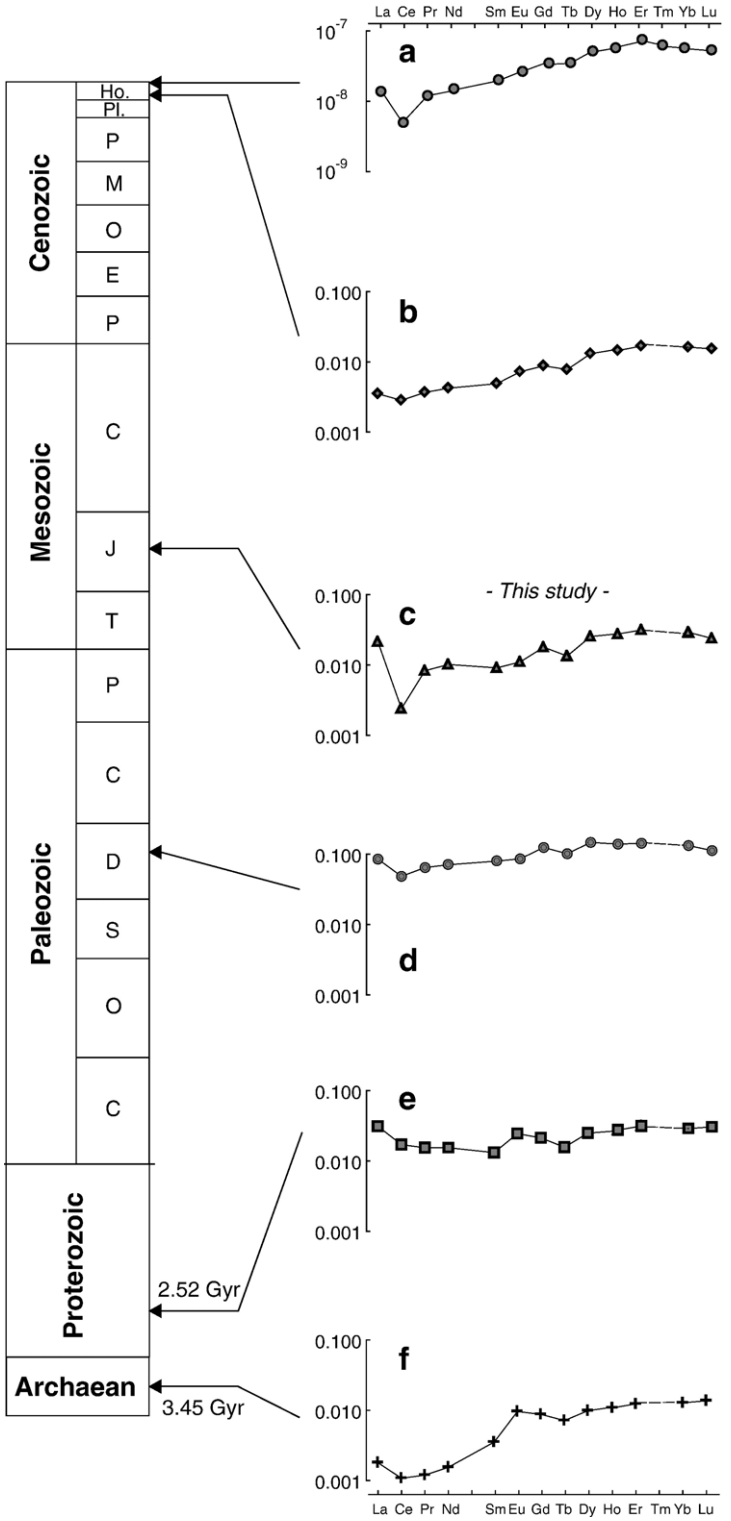
Cenozoic
Ho.
Pl.
P
M
O
E
P
Mesozoic
C
J
T
Paleozoic
P
C
D
S
O
C
Proterozoic
Archaean
2.52 Gyr
3.45 Gyr
La Ce Pr Nd Sm Eu Gd Tb Dy Ho Er Tm Yb Lu
a
b
c
d
e
f
- This study -

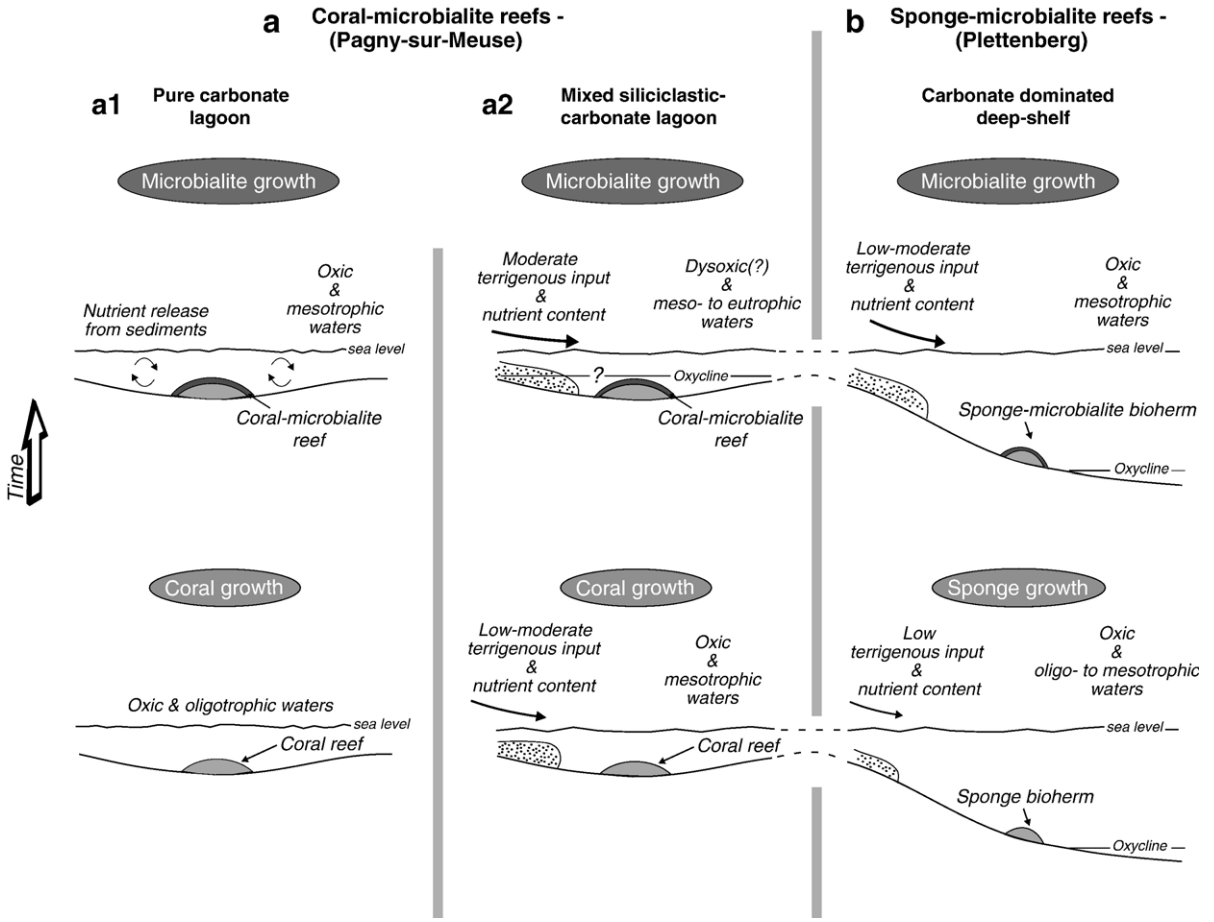

Fig. 7. Depositional models of microbialites in (a) coral-microbialite reefs of (a1) pure carbonate and (a2) mixed siliciclastic-carbonate lagoons (Pagny-sur-Meuse) and in (b) sponge-microbialite bioherms of carbonate-dominated deep shelf (Plettenberg). The main microbialite development occurred at the reef surface after the growth of a primary framework made of sponges or corals. Pagny-sur-Meuse and Plettenberg bioconstructions developed along the northwestern Tethys margin during the same time interval (Bimammatum Zone; Table 1). The Chay Peninsula microbialites, which developed on a mixed carbonate-siliciclastic ramp, are not illustrated in this figure, but is considered to reflect similar palaeoenvironmental conditions than mixed siliciclastic-carbonate lagoons of Pagny-sur-Meuse. See text for more explanation.

modern coral reefs of French Polynesia (Sprachta et al., 2001).

4. Conclusions

Results for major, rare earth elements and Nd isotopes reinforce the notion that microbialites are reliable proxies for reconstruction of ancient seawater geochemical signatures. Although collected laterally to carbonate-rich limestone levels (CaO 85–99%), the amount of siliciclastic material recorded in studied Upper Jurassic microbialites directly influences their REE composition. Even with a low contribution of terrigenous material, microbialites can lose their seawater REE signature. Lateral and intra-reef sediments, and to a lesser degree stromatolitic microbialites are more easily disturbed by

Fig. 6. Shale-normalized REE patterns for microbialites along geological times. (a) Modern seawater. The REE concentrations correspond to the average of seawater values measured between 9 and 50 m depth at different sites of the western south Pacific Ocean by Zhang and Nozaki (1996) and concentrations determined by Alibo and Nozaki (1999) at 50 m depth in the western North Pacific near Japan. (b) Holocene reefal microbialites from Australia (Webb and Kamber, 2000). The pattern represented in (c) corresponds to the average of concentrations measured in microbialites of pure carbonate setting (Pagny-sur-Meuse). (d) Late Devonian microbialites of thrombolitic fabric from Australia (Nothdurft et al., 2004). (e) Late Archaean microbialites (2.52 Ga) from South Africa (Kamber and Webb, 2001). (f) Archaean microbialites of stromatolitic fabric (3.45 Ga) from Australia (Van Kranendonk et al., 2003). Only one pattern corresponding to the mean composition has been represented for the different geological times in order to clarify the figure.

such contamination than other microbial crusts of thrombolitic fabric. With no or minor terrigenous contamination, microbialites sampled in lagoonal coral reefs (Pagny-sur-Meuse) and to a lesser degree in deep-shelf sponge bioherms (Plettenberg) record shale-normalized REE patterns characterised by a LREE depletion relative to HREE, an enrichment in HREE relative to MREE, a negative Ce anomaly, and positive La and Gd anomalies. These results imply that Upper Jurassic seawaters of the northwestern Tethys margin were characterised by REE chemistry similar to modern oceans.

REE compositions also give information on the depositional environments of microbialites in Upper Jurassic coral and sponge bioconstructions. The presence of microbialites at the reef surface, coupled with the absence of positive Ce anomalies and HREE enrichment, suggest that microbialite formation was not controlled by alkaline and high-pH ambient seawaters. The carbonate precipitation more probably occurred in microenvironments within biofilms. In both coral and sponge reefs, the development of microbialites occurred in well-oxygenated waters, probably after an increase in the nutrient content.

Acknowledgements

We are grateful to F. Albarède, R.W. Carlson, S. Guillot and P. Télouk for instrumental facilities and support. We thank P. Capiez for performing major element measurements and M. Horan for very helpful chemical advices. Constructive comments made by G. Dromart and E. Pucéat greatly improved an earlier version of the manuscript. We are grateful to B. Pittet, C. Lécuyer and F. Albarède for interesting discussions. Thoughtful comments by two anonymous reviewers are acknowledged. This research was supported by funding from the Laboratory "Paléoenvironnements et paléobiosphère" of Lyon (UMR CNRS 5125), the "Ecole Normale Supérieure" of Lyon (UMR CNRS 5570) and the Department of Terrestrial Magnetism (CIW). **[LW]**

References

Alibo, D.S., Nozaki, Y., 1999. Rare earth elements in seawater: particle association, shale-normalization, and Ce oxidation. Geochim. Cosmochim. Acta 63, 363–372.

Arp, G., Reitner, J., Wörheide, G., Landmann, G., 1996. New data on microbial communities and related sponge faune from the alkaline Satonda Crater Lake (Sumbawa, Indonesia). In: Reitner, J., Neuweiler, F., Gunkel, F. (Eds.), Global and Regional Controls on Biogenic Sedimentation, Göttingen, pp. 1–7.

Arp, G., Reimer, A., Reitner, J., 2001. Phytosynthesis-induced biofilm calcification and calcium concentrations in Phanerozoic Oceans. Science 292, 1701–1704.

Banner, J.L., Hanson, G.N., Meyers, W.J., 1988. Rare earth element and Nd isotopic variations in regionally extensive dolomites from the Burlington-Keokuk Formation (Mississippian): implications for REE mobility during carbonate diagenesis. J. Sediment. Petrol. 58, 415–432.

Bau, M., Dulski, P., 1996. Distribution of yttrium and rare-earth elements in the Penge and Kuruman iron-formations, Transvaal Supergroup, South Africa. Precambrian Res. 79, 37–55.

Bertling, M., Insalaco, E., 1998. Late Jurassic coral/microbial reefs from the northern Paris Basin-facies, palaeoecology and palaeobiogeography. Palaeogeogr. Palaeoclimatol. Palaeoecol. 139, 139–175.

Boyle, E.A., Keigwin, L.D., 1985. Comparison of Atlantic and Pacific palaeochemical record of the last 215,000 years: changes in deep ocean circulation and chemical inventories. Earth Planet. Sci. Lett. 76, 135–150.

Brand, U., Veizer, J., 1980. Chemical diagenesis of a multicomponent carbonate system: 1. Trace elements. J. Sediment. Petrol. 50, 1219–1236.

Burne, R.V., Moore, L.S., 1987. Microbialites: organosedimentary deposits of benthic microbial communities. Palaios 2, 241–254.

Byrne, R.H., Kim, K.-H., 1990. Rare earth element scavenging in seawater. Geochim. Cosmochim. Acta 54, 2645–2656.

Byrne, R.H., Kim, K.-H., 1993. Rare earth precipitation and coprecipitation behavior; the limiting role of PO (super 3-) (sub 4) on dissolved rare earth concentrations in seawater. Geochim. Cosmochim. Acta 57, 519–526.

Byrne, R.H., Sholkovitz, E.R., 1996. Marine chemistry and geochemistry of the lanthanides. In: Gschneidner, K.A.J., Eyring, L. (Eds.), Handbook on the Physics and Chemistry of Rare Earths, vol. 23. Elsevier, Amsterdam, pp. 497–593.

Camoin, G.F., Gautret, P., Montaggioni, L.F., Gabioch, G., 1999. Nature and environmental significance of microbialites in Quaternary reefs: the Tahiti paradox. Sediment. Geol. 126, 271–304.

Cantrell, K.J., Byrne, R.H., 1987. Rare earth element complexation by carbonate and oxalate ions. Geochim. Cosmochim. Acta 51, 597–605.

Carpentier, C., 2004. Géométries et environnements de dépôt de Lorraine. PhD thesis, Université Henri Poincaré, Nancy. 470 pp.

Castanier, S., Métayer-Levrel, G.L., Perthuisot, J.-P., 1999. Ca-carbonates precipitation and limestone genesis—the microbiogeologist point of view. Sediment. Geol. 126, 9–23.

Davies, S.J., Pickering, K.T., 1999. Stratigraphic control on mudrock chemistry, Kimmeridgian boulder bed succession, NE Scotland. Chem. Geol. 156, 5–23.

de Baar, H.J.W., Bacon, M., Brewer, P.G., 1985. Rare earth elements in the Pacific and Atlantic Oceans. Geochim. Cosmochim. Acta 49, 1943–1959.

Dromart, G., Gaillard, C., Jansa, L.F., 1994. Deep-marine microbial structures in the Upper Jurassic of western Téthys. In: Bertrand-Sarfati, J., Monty, C.L.V. (Eds.), Phanerozoic Stromatolites II. Kluser, Dordrecht, pp. 345–391.

Dupraz, C., Strasser, A., 1999. Microbialites and micro-encrusters in shallow coral bioherms (Middle to Late Oxfordian, Swiss Jura Mountains). Facies 40, 101–130.

Dupraz, C., Strasser, A., 2002. Nutritional modes in coral-microbialite reefs (Jurassic, Oxfordian, Switzerland). Evolution of trophic

structure as a response to environmental change. Palaios 17, 449–471.

Elderfield, H., 1988. The oceanic chemistry of the rare-earth elements. Philos. Trans. R. Soc. London, Ser. A 325, 105–126.

Geister, J., Lathuilière, B., 1991. Jurassic coral reefs of the northeastern Paris Basin (Luxembourg Lorraine). 6th International Symposium on Fossil Cnidaria including Archaeocyatha and Porifera. Excursion Guidebook. International Association for the Study of Fossil Cnidaria and Porifera, Münster. 112 pp.

German, C.R., Elderfield, H., 1990. Application of the Ce anomaly as a paleoredox indicator: the ground rules. Paleoceanography 5, 823–833.

Goldstein, S.J., Jacobsen, S.B., 1988. Rare earth elements in river waters. Earth Planet. Sci. Lett. 89, 35–47.

Govindaraju, K., 1994. Compilation of working values and descriptions for 383 geostandards. Geostand. Newsl. 18, 1–158.

Gradstein, F.M., Agterberg, F.P., Ogg, J.G., Hardenbol, J., van Veen, P., Thiery, J., Huang, Z., 1994. A Mesozoic timescale. J. Geophys. Res. 99, 24051–24074.

Grandjean, P., Cappetta, H., Albarède, F., 1987. The assessment of REE patterns and $^{143}Nd/^{144}Nd$ ratios in fish remains. Earth Planet. Sci. Lett. 84, 181–196.

Grandjean, P., Cappetta, H., Albarède, F., 1988. The REE and Nd of 40–70 Ma old fish debris from the West-African platform. Geophys. Res. Lett. 15, 389–392.

Grandjean-Lécuyer, P., Feist, R., Albarède, F., 1993. Rare earth elements in old biogenic apatites. Geochim. Cosmochim. Acta 57, 2507–2514.

Hantzpergue, P., 1991. Différentiation paléobiogéographique d'une faune d'ammonites dans l'horizon à *Ardescia pseudolictor* (zone à Cymodoce) du Kimméridgien nord-aquitain. Géobios 24, 423–433.

Haskin, M.A., Haskin, L.A., 1966. Rare earths in European shales: a redetermination. Science 154, 507–509.

Holser, W.T., 1997. Evaluation of the application of rare-earth elements to paleoceanography. Palaeogeogr. Palaeoclimatol. Palaeoecol. 132, 309–323.

Ilyin, A.V., 1998. Rare-earth geochemistry of "old" phosphorites and probability of syngenetic precipitation and accumulation of phosphate. Chem. Geol. 144, 243–256.

Kamber, B.S., Webb, G.E., 2001. The geochemistry of Late Archaean microbial carbonate: implications for ocean chemistry and continental erosion history. Geochim. Cosmochim. Acta 65, 2509–2525.

Kamber, B.S., Bolhar, R., Webb, G.E., 2004. Geochemistry of Late Archaean stromatolites from Zimbabwe: evidence for microbial life in restricted epicontinental seas. Precambrian Res. 132, 379–399.

Kempe, S., Degens, E.T., 1985. An early soda ocean? Chem. Geol. 53, 95–108.

Kempe, S., Kazmierczak, J., Reimer, A., Landmann, G., Reitner, J., 1996. Microbialites and hydrochemistry of the Crater Lake of Satonda—a status report. In: Reitner, J., Neuweiler, F., Gunkel, F. (Eds.), Global and Regional Controls on Biogenic Sedimentation. Research Reports, Gött. Arb. Geol. Paläontol. Sb., vol. 2, pp. 59–63.

Keupp, H., Jenisch, A., Herrmann, R., Neuweiler, F., Reitner, J., 1993. Microbial carbonate crusts—a key to the environmental analysis of fossil spongiolites? Facies 29, 41–54.

Lathuilière, B., Carpentier, C., André, G., Dagallier, G., Durand, M., Hanzo, M., Huault, V., Harmand, D., Hibsch, C., Le Roux, J., Malartre, F., Martin-Garin, B., Nori, L., 2003. Production carbonatée dans le Jurassique de Lorraine. Excursion Guide Book. GFEJ, Nancy, 115 pp.

Lécuyer, C., Reynard, B., Grandjean, P., 2004. Rare earth element evolution of Phanerozoic seawater recorded in biogenic apatites. Chem. Geol. 204, 63–102.

Leinfelder, R.R., 2001. Jurassic reef ecosystems. In: Stanley Jr., G.D. (Ed.), The History and Sedimentology of Ancient Reef Systems. Kluwer Academic/Plenum Publishers, New York, pp. 251–302.

Leinfelder, R.R., Schmid, D.U., 2000. Mesozoic reefal thrombolites and other microbolites. In: Riding, R.E., Awramik, S.M. (Eds.), Microbial Sediments. Springer, Berlin, pp. 289–294.

Leinfelder, R.R., Nose, M., Schmid, D.U., Werner, W., 1993. Microbial crusts of the Late Jurassic: composition, palaeoecological significance and importance in reef construction. Facies 29, 195–230.

Leinfelder, R.R., Krautter, M., Laternser, R., Nose, M., Schmid, D.U., Schweigert, G., Werner, W., Keupp, H., Brugger, H., Herrmann, R., Rehfeld-Kiefer, U., Schroeder, J.H., Reinhold, C., Koch, R., Zeiss, A., Schweizer, V., Christmann, H., Menges, G., Luterbacher, H., 1994. The origin of Jurassic reefs. Current research developments and results. Facies 31, 1–56.

Leinfelder, R.R., Werner, W., Nose, M., Schmid, D.U., Krautter, M., Laternser, R., Takacs, M., Hartmann, D., 1996. Paleoecology, growth parameters and dynamics of coral, sponge and microbolite reefs from the Late Jurassic. In: Reitner, J., Neuweiler, F., Gunkel, F. (Eds.), Global and Regional Controls on Biogenic Sedimentation. Research Reports, Gött. Arb. Geol. Paläontol. Sb., vol. 2, pp. 227–248.

Liu, Y.-G., Miah, M.R.U., Schmitt, R.A., 1988. Cerium: a chemical tracer for palaeo-oceanic redox conditions. Geochim. Cosmochim. Acta 52, 1361–1371.

McArthur, J.M., Walsh, J.N., 1984. Rare-earth geochemistry of phosphorites. Chem. Geol. 47, 191–220.

McCook, L.J., 2001. Competition between corals and algal turfs along a gradient of terrestrial influence in the nearshore central Great Barrier Reef. Coral Reefs 19, 419–425.

Meyer, R.K.L., Schmidt-Kaler, H., 1990. Palaeogeography and development of sponge reefs in the Upper Jurassic of southern Germany—an overview. Facies 23, 175–184.

Möller, P., Bau, M., 1993. Rare-earth patterns with positive cerium anomaly in alkaline waters from Lake Van, Turkey. Earth Planet. Sci. Lett. 117, 671–676.

Murray, R.W., Buchholtz Ten Brink, M.R., Jones, D.L., Gerlach, D.C., Price Russ III, G., 1990. Rare earth elements as indicators of different marine depositional environments in chert and shale. Geology 18, 268–271.

Murray, R.W., Buchholtz Ten Brink, M.R., Gerlach, D.C., Price Russ III, G., Jones, D.L., 1991. Rare earth, major, and trace elements in chert from the Franciscan Complex and Monterey Group, California: assessing sources to fine-grained marine sediments. Geochim. Cosmochim. Acta 55, 1875–1895.

Nothdurft, L.D., Webb, G.E., Kamber, B.S., 2004. Rare earth element geochemistry of Late Devonian reefal carbonates, Canning Basin, western Australia: confirmation of a seawater REE proxy in ancient limestones. Geochim. Cosmochim. Acta 68, 263–283.

Nothdurft, L.D., Webb, G.E., Buster, N.A., Holmes, C.W., Sorauf, J. E., Kloproge, J.T., 2005. Brucite microbialites in living coral skeletons: indicators of extreme microenvironments in shallow-marine settings. Geology 33, 161–240.

Olivier, N., 2004. Microbialites dans les bioconstructions du Jurassique: morphologies, rôles édificateurs et significations paléoenvironnementales. PhD thesis, Université Claude Bernard Lyon1, Lyon. 381 pp.

Olivier, N., Hantzpergue, P., Gaillard, C., Pittet, B., Leinfelder, R., Schmid, D.U., Werner, W., 2003. Microbialite morphology, structure and growth: a model of the Upper Jurassic reefs of the Chay Peninsula (western France). Palaeogeogr. Palaeoclimatol. Palaeoecol. 193, 383–404.

Olivier, N., Carpentier, C., Martin-Garin, B., Lathuilière, B., Gaillard, C., Ferry, S., Hantzpergue, P., Geister, J., 2004a. Coral-microbialite reefs in pure carbonate versus mixed carbonate-siliciclastic depositional environments: the example of the Pagny-sur-Meuse section (Upper Jurassic; northeastern France). Facies 50, 229–255.

Olivier, N., Pittet, B., Mattioli, E., 2004b. Palaeoenvironmental control on sponge-microbialite reefs and contemporaneous deep-shelf marl-limestone deposition (Late Oxfordian, southern Germany). Palaeogeogr. Palaeoclimatol. Palaeoecol. 212, 233–263.

Picard, S., Lécuyer, C., Barrat, J.-A., Garcia, J.-P., Dromart, G., Sheppard, S.M.F., 2002. Rare earth element contents of Jurassic fish and reptile teeth and their potential relation to seawater composition (Anglo-Paris Basin, France and England). Chem. Geol. 186, 1–16.

Pichat, S., 2001. Variations du rapport (^{231}Pa/^{230}Th)XS,O et de la composition isotopique du zinc dans des sédiments de l'océan Pacifique équatorial au Quaternaire. Implications pour la productivité biologique et relations avec la thermocline. PhD thesis, Ecole Normale Supérieure, Lyon. 222 pp.

Piepgras, D.J., Jacobsen, S.B., 1992. The behaviour of rare earth elements in seawater: precise determination of variations in the North Pacific water column. Geochim. Cosmochim. Acta 56, 1851–1862.

Pin, C., Zalduegui, J.F.S., 1997. Sequential separation of light rare-earth elements, thorium and uranium by miniaturized extraction chromatography: application to isotopic analyses of silicate rocks. Anal. Chim. Acta 339, 79–89.

Piper, D.Z., 1974. Rare earth elements in the sedimentary cycle: a summary. Chem. Geol. 14, 285–304.

Pittet, B., Mattioli, E., 2002. The carbonate signal and calcareous nannofossil distribution in an Upper Jurassic section (Balingen-Tieringen, Late Oxfordian, southern Germany). Palaeogeogr. Palaeoclimatol. Palaeoecol. 179, 71–96.

Pittet, B., Strasser, A., 1998. Depositional sequences in deep-shelf environments formed through carbonate-mud import from the shallow platform (Late Oxfordian, German Swabian Alb and eastern Swiss Jura). Eclogae Geol. Helv. 91, 149–169.

Reitner, J., 1993. Modern cryptic microbialite/metazoan facies from Lizard Island (Great Barrier Reef, Australia): formation and concepts. Facies 29, 3–40.

Reitner, J., Neuweiler, F., 1995. Supposed principal controlling factors of rigid micrite buildups. In: Reitner, J., Neuweiler, F. (Eds.), Mud Mounds: Polygenetic Spectrum of Fine-Grained Carbonate BuildupsFacies, vol. 32, pp. 62–65.

Reynard, B., Lécuyer, C., Grandjean, P., 1999. Crystal-chemical controls on rare-earth element concentrations in fossil biogenic apatites and implications for palaeoenvironmental reconstructions. Chem. Geol. 155, 233–241.

Riding, R., 2000. Microbial carbonates: the geological record of calcified bacterial–algal mats and biofilms. Sedimentology 47, 179–214.

Riding, R., 2005. Phanerozoic reefal microbial carbonate abundance: comparisons with metazoan diversity, mass extinction events, and seawater saturation state. Rev. Esp. Micropaleontol. 37, 23–39.

Riding, R., Liang, L., 2005a. Seawater chemistry control of marine limestone accumulation over the past 550 million years. Rev. Esp. Micropaleontol. 37, 1–11.

Riding, R., Liang, L., 2005b. Geobiology of microbial carbonates: metazoan and seawater saturation state influences on secular trends during the Phanerozoic. Palaeogeogr. Palaeoclimatol. Palaeoecol. 219, 101–115.

Roth, P.H., 1986. Mesozoic palaeoceanography of the North Atlantic and Tethys Oceans. Spec. Publ.-Geol. Soc. Lond. 21, 299–320.

Schmid, D.U., 1996. Marine microbolites and micro-encrusters from the Upper Jurassic. Profil 9, 101–251.

Schmid, D.U., Leinfelder, R.R., Nose, M., 2001. Growth dynamics and ecology of Upper Jurassic mounds, with comparisons to Mid-Palaeozoic mounds. Sediment. Geol. 145, 343–376.

Shaw, H.F., Wasserburg, G.J., 1985. Sm–Nd in marine carbonates and phosphates: implications for Nd isotopes in seawater and crustal ages. Geochim. Cosmochim. Acta 49, 503–518.

Shields, G.A., Stille, P., 2001. Diagenetic constraints on the use of cerium anomalies as palaeoseawater redox proxies: an isotopic and REE study of Cambrian phosphorites. Chem. Geol. 175, 29–48.

Shields, G.A., Webb, G.E., 2004. Has the REE composition of seawater changed over geological time? Chem. Geol. 204, 103–107.

Sholkovitz, E.R., Shaw, T.J., Schneider, D.L., 1996. The geochemistry of rare earth elements in the seasonally anoxic water column and porewaters of Chesapeake Bay. Geochim. Cosmochim. Acta 56, 3389–3402.

Sprachta, S., Camoin, G., Golubic, S., Campion, T.L., 2001. Microbialites in a modern lagoonal environment: nature and distribution, Tikehau atoll (French Polynesia). Palaeogeogr. Palaeoclimatol. Palaeoecol. 175, 103–124.

Stille, P., Clauer, N., Abrecht, J., 1989. Nd isotopic composition of Jurassic Tethys seawater and the genesis of Alpine Mn-deposits: evidence from Sr–Nd isotope data. Geochim. Cosmochim. Acta 53, 1095–1099.

Stille, P., Steinmann, M., Riggs, S.R., 1996. Nd isotope evidence for the evolution of the palaeocurrents in the Atlantic and Tethys Oceans during the past 180 Ma. Earth Planet. Sci. Lett. 144, 9–19.

Thompson, J.B., Ferris, F.G., Smith, D.A., 1990. Geomicrobiology and sedimentology of the mixolimnion and chemocline in Fayetteville Green Lake, New York. Palaios 5, 52–75.

Van Kranendonk, M., Webb, G.E., Kamber, B.S., 2003. Geological and trace evidence for a marine sedimentary environment of deposition and biogenicity of 3.45 Ga stromatolitic carbonates in the Pilbara Craton, and support for a reducing Archaean ocean. Geobiology 1, 91–108.

Webb, G.E., 2001. Biologically induced carbonate precipitation in reefs through time. In: Stanley Jr., G.D. (Ed.), The History and Sedimentology of Ancient Reef Systems. Kluwer Academic/Plenum Publishers, New York, pp. 159–203.

Webb, G.E., Kamber, B.S., 2000. Rare earth elements in Holocene reefal microbialites: a new shallow seawater proxy. Geochim. Cosmochim. Acta 64, 1557–1565.

Wood, R.A., 1999. Reef Evolution. Oxford University Press. 414 pp.

Woolfe, K.J., Larcombe, P., 1998. Terrigenous sediment accumulation as a regional control on the distribution of reef carbonates. In: Camoin, G.F., Davies, P.J. (Eds.), Reefs and Carbonate Platforms

in the Pacific and Indian Oceans. Spec. Publ. Int. Assoc. Sedimentol., vol. 25, pp. 295–310.

Wright, J., Schrader, H., Hosler, W.T., 1987. Palaeoredox variations in ancient oceans recorded by rare earth elements in fossil apatite. Geochim. Cosmochim. Acta 51, 631–644.

Zhang, J., Nozaki, Y., 1996. Rare earth elements and yttrium in seawater: ICP-MS determinations in the East Caroline, Coral Sea, and South Fiji basins of the western South Pacific Ocean. Geochim. Cosmochim. Acta 60, 4631–4644.

Ziegler, P.A., 1990. Pangaea break-up: Jurassic–Early Cretaceous opening of central Atlantic and western Tethys. In: Ziegler, P.A. (Ed.), Geological Atlas of Western and Central Europe (second and completely revised edition). Shell Intern. Petr. Maatschappij B.V., Amsterdam, pp. 91–122.